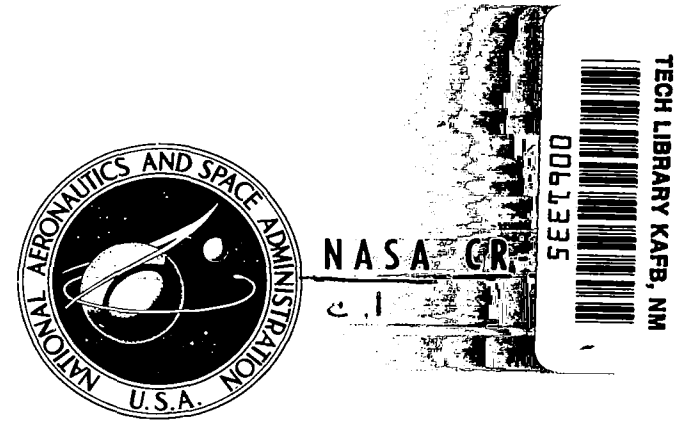

NASA CONTRACTOR REPORT

NASA CR-2025

THE ROLE OF GRAIN SIZE AND SHAPE IN THE STRENGTHENING OF DISPERSION HARDENED NICKEL ALLOYS

by B. A. Wilcox and A. H. Clauer

Prepared by
BATTELLE
Columbus, Ohio 43201
for Lewis Research Center

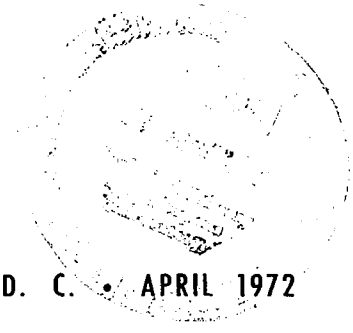

NATIONAL AERONAUTICS AND SPACE ADMINISTRATION • WASHINGTON, D. C. • APRIL 1972

1. Report No.	2. Government Accession No.	3. Recipient's Catalog No.
CR-2025		

4. Title and Subtitle	5. Report Date
THE ROLE OF GRAIN SIZE AND SHAPE IN THE STRENGTHENING OF DISPERSION HARDENED NICKEL ALLOYS	April 1972
	6. Performing Organization Code

7. Author(s)	8. Performing Organization Report No.
B. A. Wilcox and A. H. Clauer	V6803
	10. Work Unit No.

9. Performing Organization Name and Address	11. Contract or Grant No.
Battelle 505 King Avenue Columbus, Ohio 43201	NAS 3-11167
	13. Type of Report and Period Covered
12. Sponsoring Agency Name and Address	Contractor Report
National Aeronautics and Space Administration Washington, D.C. 20546	14. Sponsoring Agency Code

15. Supplementary Notes

Project Managers, Thomas K. Glasgow, Fredric H. Harf, and Charles W. Andrews, Materials and Structures Division, NASA Lewis Research Center, Cleveland, Ohio

16. Abstract

Thermomechanical processing was used to develop various microstructures in Ni, Ni-2Th0_2, Ni-20Cr, Ni-20Cr-2Th0_2, Ni-20Cr-10W, and Ni-20Cr-10W-2Th0_2. The yield strength at 25^{o} C increased with substructure refinement according to the Hall-Petch relation, and substructure refinement was a much more potent means of strengthening than was dispersion hardening. At elevated temperature (1093^{o} C), the most important microstructural feature affecting strength was the grain aspect ratio (grain length, L, divided by grain width, ℓ). The yield strength and creep strength increased linearly with increasing L/ℓ, obeying the relation

$$\sigma = \sigma_e + K(L/\ell - 1)$$

where σ_e = strength at $L/\ell = 1$ (equiaxed grains) and K = a constant. The significance of this equation relates to grain boundary sliding, the major mode of high temperature deformation.

17. Key Words (Suggested by Author(s))	18. Distribution Statement
Grain aspect ratio Dispersion strengthening Thoriated Ni alloys Substructure strengthening	Unclassified - unlimited

19. Security Classif. (of this report)	20. Security Classif. (of this page)	21. No. of Pages	22. Price*
Unclassified	Unclassified	29	$3.00

* For sale by the National Technical Information Service, Springfield, Virginia 22151

1. Nickel alloys -- mechanical properties -
2. Grain size -

1972

TABLE OF CONTENTS

THE ROLE OF GRAIN SIZE AND SHAPE IN THE STRENGTHENING OF DISPERSION HARDENED NICKEL ALLOYS

by

B. A. Wilcox and A. H. Clauer

SUMMARY

Thermomechanical processing (TMP) by drawing and swaging have been used to work three dispersion strengthened Ni alloys and their dispersion-free counterparts: Ni-2ThO_2, Ni, Ni-20Cr-2ThO_2, Ni-20Cr, Ni-20Cr-10W-2ThO_2, and Ni-20Cr-10W. The purpose was to examine the important features of indirect strengthening due to dispersed particles, and this was done by evaluating how TMP influenced microstructure, tensile deformation behavior at 25 and 1093 °C and creep behavior at 1093 °C.

Room temperature strength was increased by TMP as a result of refining the grain size and substructure spacing (cell size), ℓ, in accord with the usual Hall-Petch relation. This substructure strengthening increment was five to six times greater than the strength increment due to particles alone.

At high temperatures (1093 °C) no good correlation was found between yield strength and grain or cell size. Instead, there was an excellent correlation between yield strength and grain aspect ratio (grain length, L, divided by grain width, ℓ), whereby the yield strength increased linearly with L/ℓ. This correlation held for nonrecrystallized Ni-2ThO_2 with very fine elongated grains, as well as recrystallized Ni-2ThO_2 which had very coarse elongated grains. The same aspect ratio correlation was found for minimum creep rate and 100-hour rupture life. This influence of grain aspect ratio was interpreted in terms of how L/ℓ influenced grain boundary sliding, which appears to be the major mode of tensile yielding and creep at 1093 °C. When the stress axis is parallel to the elongated grain direction, increasing L/ℓ lowers the resolved shear stress on boundaries, on average, and this minimizes the overall amount of sliding.

Thus, a fine, stable, very elongated grain structure is optimum for combined room temperature and high temperature strengthening, and this can be achieved in Ni-2ThO_2 bar, but apparently not in Cr-containing alloys. Here recrystallization occurs at high temperatures, sometimes giving fine, nearly equiaxed, grains and sometimes coarse elongated grains.

INTRODUCTION

Various workers have attributed dispersion strengthening of nickel alloys to the Orowan mechanism of hardening by nondeforming particles.[1-5] However, in addition to this "direct strengthening" by second phase particles it is possible to thermomechanically process (TMP) such alloys to develop additional strength at room temperature and elevated temperatures. Various effects of TMP on Ni-ThO_2 base alloys have been studied by numerous researchers[4, 6-12], and in particular a large effort has been directed toward investigating how TMP influences recovery and recrystallization behavior[6, 7, 10, 11, 13-21] as well as mechanical properties. Second phase particles play a role in the microstructure and attendant strengthening produced by TMP and here the effects of particles have been termed "indirect strengthening".[22]

It was the purpose of the present study to thermomechanically process dispersion strengthened nickel alloys and their dispersion free counterparts to produce various microstructures. By examining how particles influence microstructural development and strength, it was intended to provide a quantitative assessment of the "indirect strengthening" contributions of ThO_2 particles in Ni-base alloys.

MATERIALS AND PROCEDURES

Materials

The six alloys studied in this investigation were obtained from Fansteel Metallurgical Corporation in the form of 0.35 to 0.40 inch (0.89-1.02 cm) diameter hot extruded bar. The chemical compositions are given in Table 1, and the ThO_2 particle sizes and spacings are listed in Table 2. The Ni, Ni-2ThO_2, Ni-20Cr, and Ni-20Cr-2ThO_2 alloys were obtained in the as-extruded condition, and the two tungsten containing alloys had been annealed for one hour at 1316 °C. The sintered billets were canned in mild steel and extruded from 2 inch (5.08 cm) diameter to 1/2 inch (1.27 cm) diameter at 1093 °C.

TABLE 1. COMPOSITION OF EXPERIMENTAL ALLOYS (WEIGHT-PERCENT)

Alloy	ThO_2	Cr	W	C	S	N
Ni	--	--	--	0.0010	0.0062	--
Ni-2ThO_2	2.9	--	--	0.0024	0.0022	0.010
Ni-20Cr	--	19.7	--	0.0278	0.0019	--
Ni-20Cr-2ThO_2	2.0	20.2	--	0.0249	0.020	0.0051
Ni-20Cr-10W	--	20.4	8.6	0.0310	0.0063	--
Ni-20Cr-10W-2ThO_2	2.8	20.8	9.9	0.0271	0.0035	--

TABLE 2. ThO_2 PARTICLE SIZES AND SPACINGS IN EXPERIMENTAL ALLOYS

Alloy	Volume Percent ThO_2	Range[(a)] of Particle Diameter, μm	Average Particle Diameter, μm	Mean Planar Center-to-Center Particle Spacing, μm
Ni-2ThO_2	2.58	0.0093-0.1163	0.0201	0.1505
Ni-20Cr-2ThO_2	1.70	0.0093-0.1128	0.0176	0.1595
Ni-20Cr-10W-2ThO_2	2.51	0.0093-0.1197	0.0192	0.1670

(a) 2000 particles were measured from transmission electron micrographs using a Zeiss Particle Size Analyzer. Particle spacings were determined as in Reference 2.

Procedures

Thermomechanical Processing

Two types of working, drawing and swaging, were used to process the alloys. Two working procedures were employed, one with no intermediate anneals (hereafter referred to as Procedure A) and the other with intermediate anneals for one hour at 1200°C in a hydrogen atmosphere (hereafter referred to as Procedure B). Only wire drawing was used to process the Ni and Ni-2ThO_2 materials, but swaging was used in some cases for the Cr-containing alloys which proved to be very difficult to work by drawing. Summarized below are the TMP conditions employed for each of the alloys.

(a) Ni and Ni-2ThO_2: Drawing by Procedure A (no intermediate anneals). Drawing by Procedure B (intermediate anneals after each 50% reduction in area).

(b) Ni-20Cr and Ni-20Cr-2ThO_2: Drawing and swaging by Procedure A (no intermediate anneals). Drawing and swaging by Procedure B (intermediate anneals after each 25% reduction in area).

(c) Ni-20Cr-10W and Ni-20Cr-10W-2ThO_2: Swaging by Procedure B only (intermediate anneals after each 25% reduction in area).

Both drawing and swaging were performed on materials preheated to 200 °C, and a teflon lubricant was used for wire drawing. The starting point for Procedure B was extruded plus annealed material. For the alloys drawn or swaged by Procedure B, all studies (microstructure, tensile, and creep tests) were made after annealing.

Tensile and Creep Testing

Tensile deformation was done in an Instron at a strain rate of 0.01 min^{-1}. Two test temperatures, 25 and 1093 °C, were used and the high temperature tests were performed in a vacuum Brew furnace attached to the Instron. The specimens had threaded ends, and those machined from rod of $\geq$ 0.25 inch (0.635 cm) diameter had a 1 inch (2.54 cm) gage length. Specimens machined from smaller diameter rods (to 0.096 inch [0.244 cm] diameter) had a 1/2 inch (1.27 cm) gage length. Axial alignment of all tests was assured by universal joints.

Tension creep tests were made on only the three ThO_2-containing alloys, and at one temperature, 1093 °C. The creep specimens had the same configuration as tensile specimens and they were tested in a vacuum of 10^{-5} torr (1.33×10^{-3} N/m^2) under constant stress conditions. Additional details of the creep testing procedures have been reported previously.[23]

RESULTS

Microstructures

The microstructures of as-extruded Ni and Ni-2ThO_2 are shown in Figure 1, and Figure 2 illustrates the as-extruded structure of Ni-20Cr and Ni-20Cr-2ThO_2. Annealing these alloys for 1 hour at 1200°C caused the grains in Ni and Ni-20Cr to coarsen. The Ni-2ThO_2 did not recrystallize but the Ni-20Cr-2ThO_2 alloy recrystallized with a fine nearly equiaxed grain structure similar to that of the extruded Ni-20Cr (Figure 2a). The annealed Ni-20Cr-10W and Ni-20Cr-10W-2ThO_2 alloys were both recrystallized, the former with a structure similar to that in Figure 2a. The recrystallized Ni-20Cr-10W-2ThO_2 had a coarser more elongated grain structure.

Drawing or swaging by Procedure A induced a dislocation substructure consisting of closed elongated cells, with the spacing between the elongated cell walls decreasing with increasing working. This is illustrated in Figure 3 for Ni and Ni-2ThO_2 drawn various amounts. The cold working opened voids at the particle/matrix interface of the thoriated alloys, and the voids elongated with increasing drawing strain. Such voids have been observed previously in Ni-ThO_2 alloys[4, 13, 24-26], and they heal during high temperature annealing.

When drawn or swaged by Procedure B, all of the alloys, except Ni-2ThO_2, recrystallized during each anneal at 1200°C, with nearly equiaxed and usually fairly fine grains. The anneals caused the Ni-2ThO_2 to recover such that the spacing between cells was approximately constant (~0.8 to 1 μm). Typical microstructures of Ni-2ThO_2 and Ni-20Cr-2ThO_2 processed by Procedure B are shown in Figure 4. Here there is an absence of voids at the particle/matrix interface and the dislocation density is relatively low, compared with alloys worked equivalent amounts by Procedure A.

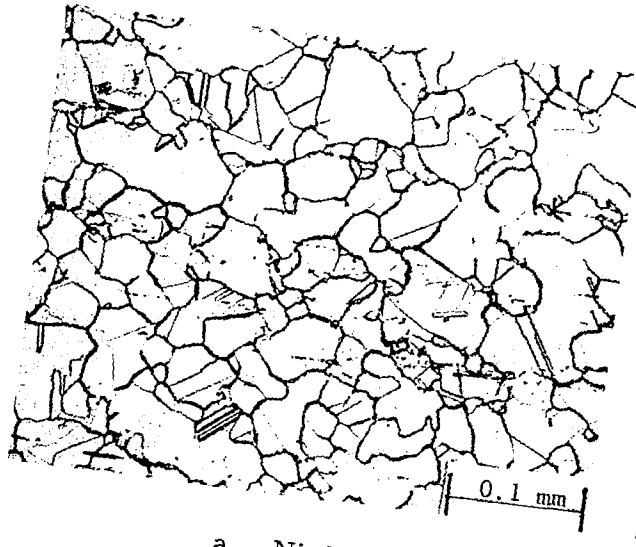

a. Nickel

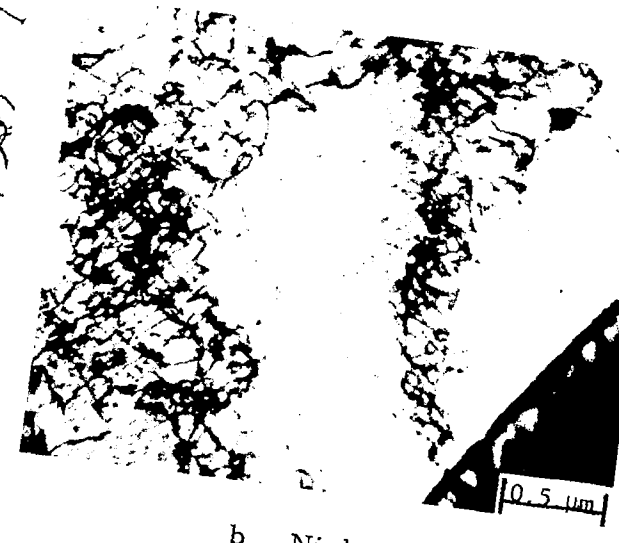

b. Nickel

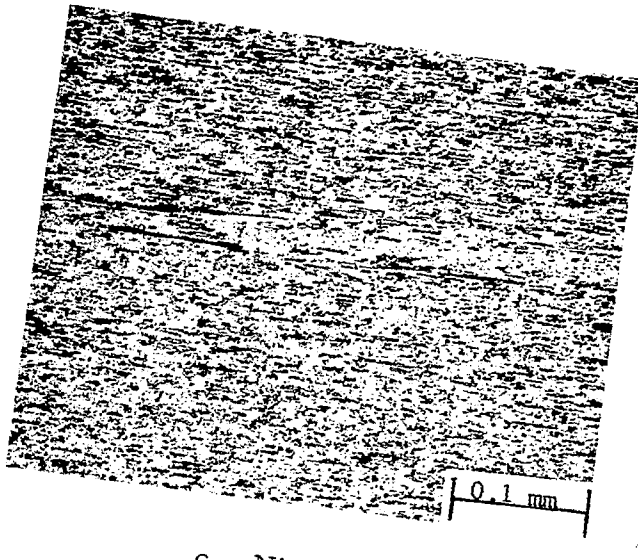

c. $Ni-2ThO_2$

d. $Ni-2ThO_2$

FIGURE 1. MICROSTRUCTURES OF AS-EXTRUDED Ni AND $Ni-2ThO_2$

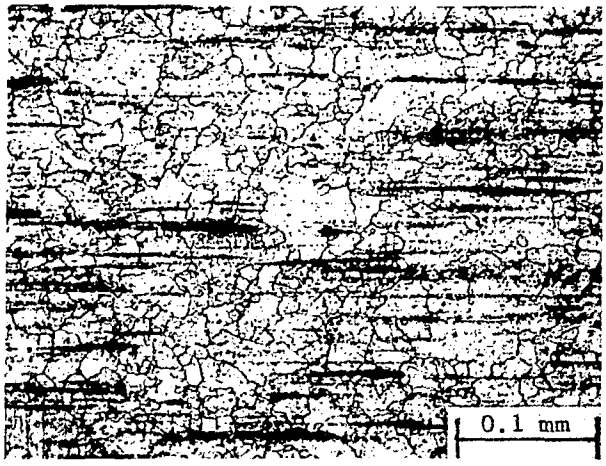

a. Ni-20Cr

b. Ni-20Cr

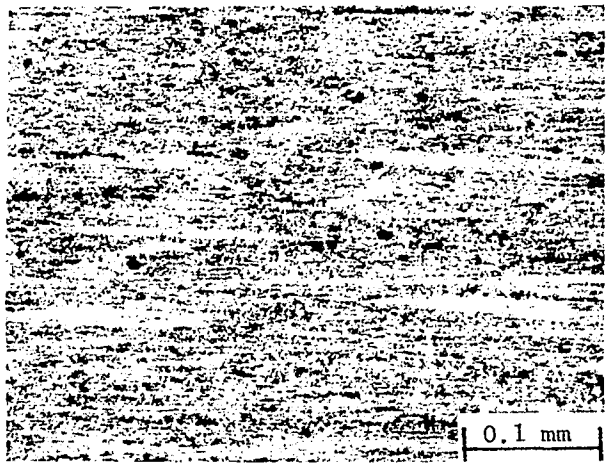

c. Ni-20Cr-2ThO_2

d. Ni-20Cr-2ThO_2

FIGURE 2. MICROSTRUCTURES OF AS-EXTRUDED Ni-20Cr AND Ni-20Cr-2ThO_2

The dark stringers in a. and c. are coarse Cr_2O_3 particles.

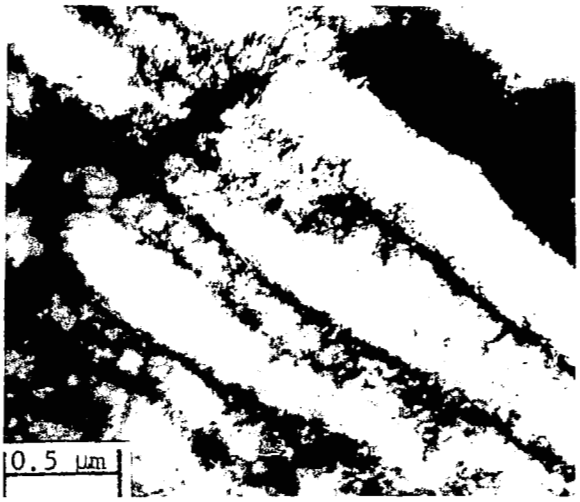

a. Nickel, Drawn 53.4%

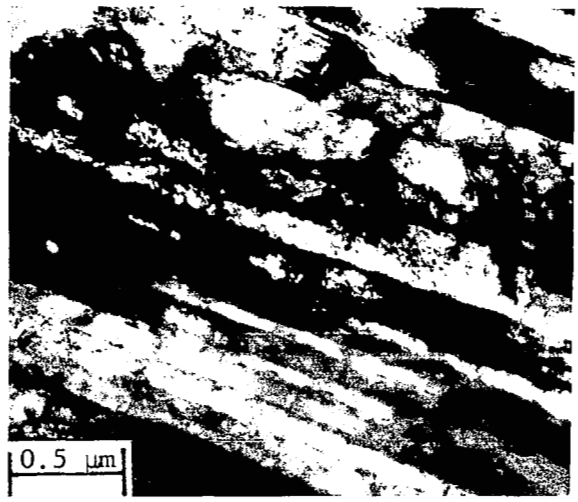

b. Nickel, Drawn 93.4%

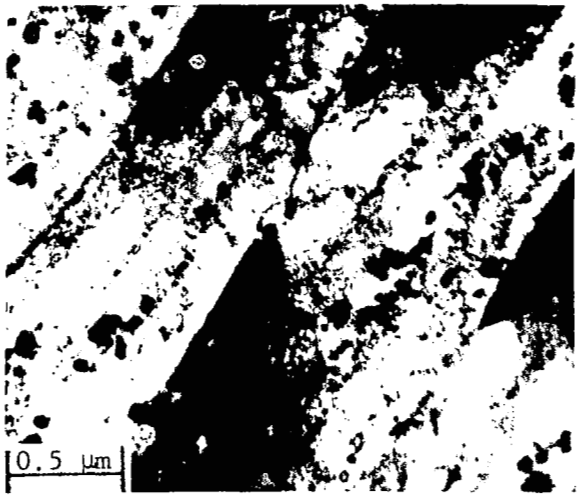

c. Ni-2ThO_2, Drawn 49.4%

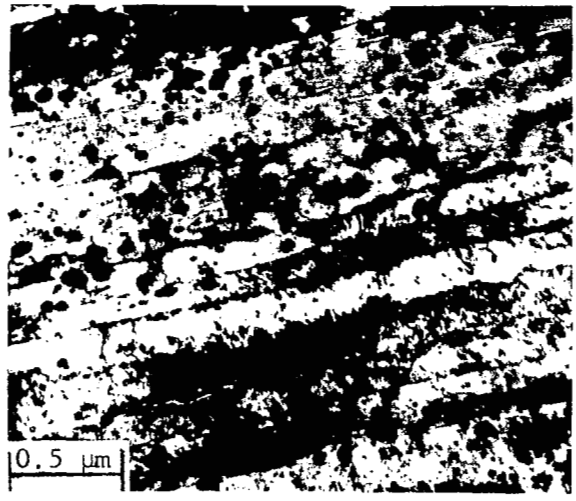

d. Ni-2ThO_2, Drawn 92.5%

FIGURE 3. INFLUENCE OF DRAWING BY PROCEDURE A (NO INTERMEDIATE ANNEALS) ON THE SUBSTRUCTURE DEVELOPED IN Ni AND Ni-2ThO_2

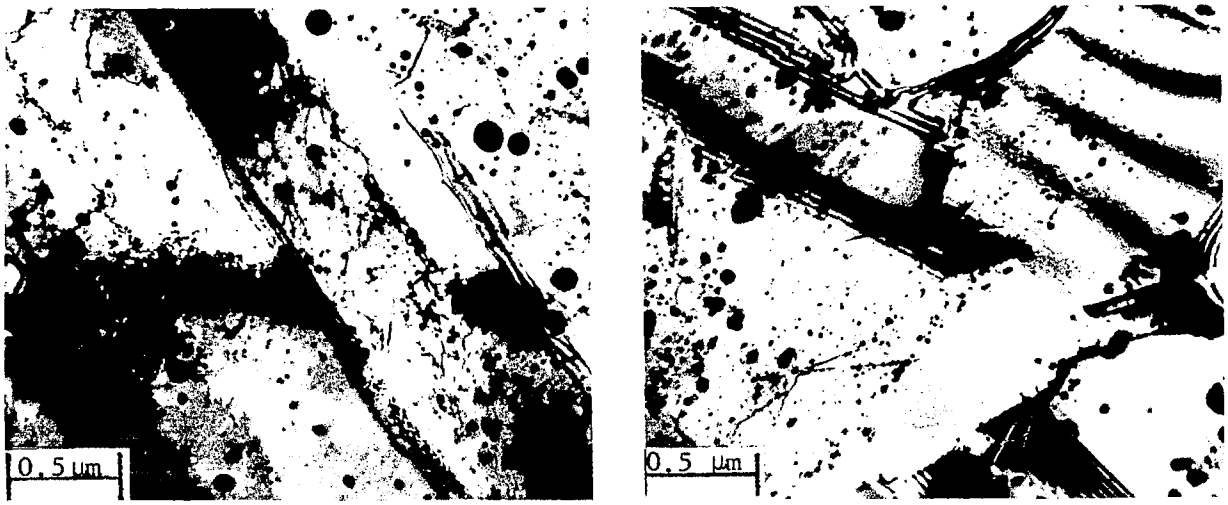

a. Ni-2ThO_2 Drawn 46.5% and Annealed 1 Hour at 1200°C

b. Ni-20Cr-2ThO_2 Drawn 25.6% and Annealed 1 Hour at 1200°C

FIGURE 4. MICROSTRUCTURES OF THORIATED ALLOYS DRAWN BY PROCEDURE B

Tensile Deformation

The room temperature strength and ductility of Ni and Ni-2ThO_2 drawn by Procedures A and B are shown in Figure 5 as a function of percent reduction by drawing, and similar results were obtained for the four Cr-containing alloys. After drawing by Procedure A (no intermediate anneals) the yield and ultimate strengths increased with increasing drawing strain. This is in accord with previous observations on drawn ferrous alloys[27-30], Mo-TZM[31], and W[32], where it has been shown that the strengthening arises from substructure refinement. The same explanation is relevant here, e.g., see Figure 3. A similar strengthening effect in drawn thoriated nickel has been reported by Worn and coworkers[6, 7]. When pure Ni was drawn by Procedure B, recrystallization occurred after each anneal, and thus the room temperature strengths in Figure 5 remained relatively constant. The slight variation in yield strength resulted mainly from a variation in the recrystallized grain size. Similarly, the strength of Ni-2ThO_2 drawn by Procedure B was nearly constant, since recovery to a cell width of 0.8 to 1 μ occurred during each anneal.

Tensile results on pure Ni and Ni-2ThO_2 at 1093°C are shown in Figure 6. There is little difference in the strength of pure Ni drawn by Procedures A and B, because specimens drawn by Procedure A recrystallized

during heat-up to the test temperature and during tensile deformation. In Figure 6 it is seen that the yield and ultimate strength of Ni-2ThO_2 at 1093 °C increase with increasing drawing strain after drawing by both Procedures A and B. The highest strengths were achieved for specimens drawn by Procedure A. The specimen drawn 92.5% by Procedure A was examined metallographically after tensile testing at 1093 °C and it had not recrystallized. A somewhat surprising observation in Figure 6 is that although there was no large variation in cell width, the strength of the Ni-2ThO_2 drawn by Procedure B increased with increasing drawing strain; but as expected, the room temperature strength was relatively constant (Figure 5). An explanation of this behavior is given later.

Creep Studies

In the creep investigation only the thoriated alloys processed by Procedure B were studied, and the final anneal at 1200 °C prior to creep produced stable microstructures in these alloys. The creep results are plotted in Figure 7 as log $\dot{\epsilon}_{min}$ versus log stress and in Figure 8 as log t_r versus log stress, where $\dot{\epsilon}_{min}$ is the minimum creep rate and t_r is the time to rupture. In both Figures 7 and 8 linear relations are apparent, which lead to the proportionalities:

$$\dot{\epsilon}_{min} \propto \sigma^{n} \quad , \tag{1}$$

and

$$t_r \propto \sigma^{-m} \quad . \tag{2}$$

The values of minimum creep rate times rupture life were found to obey the usual empirical relation:

$$\dot{\epsilon}_{min} \cdot t_r \approx C \quad , \tag{3}$$

and the average value for C from all tests was $\sim 10^{-2}$. Thus, for example, a rough estimate of the minimum creep rate for material which ruptures after 100 hours at 1093 °C would be $\dot{\epsilon}_{min} = 10^{-4}\ hr^{-1}$.

For Ni-2ThO_2 (Figures 7a and 8a) increasing the amount of total reduction by drawing Procedure B had two effects: (1) the plots are shifted to higher stresses for a given $\dot{\epsilon}_{min}$ or t_r and (2) the slopes (n and m values) increase. The exponents increased from 6.7 to 26.1 for minimum creep rate (Figure 7a) and from 7.8 to 19.6 for rupture life (Figure 8a). Stress

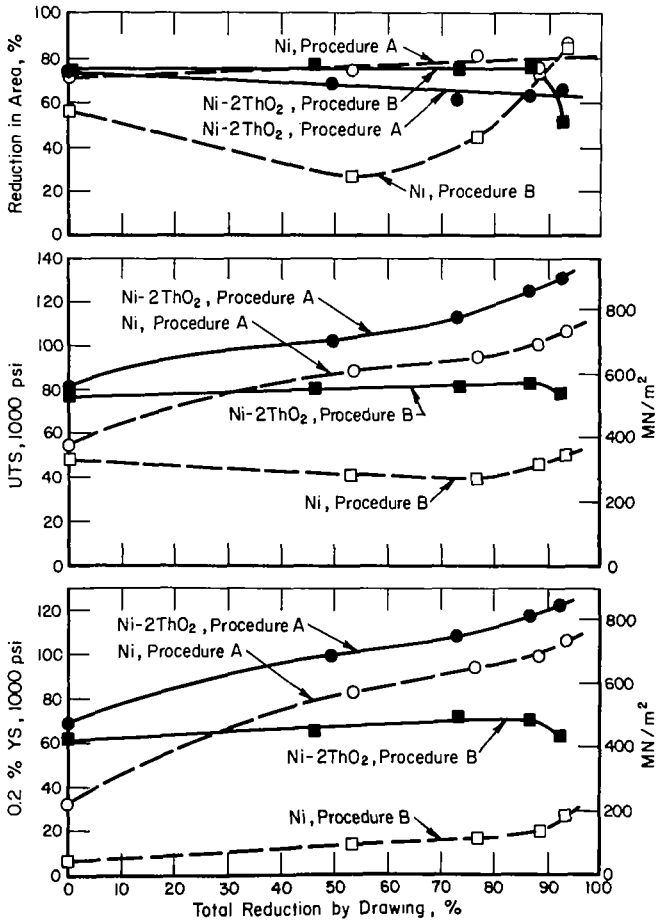

FIGURE 5. INFLUENCE OF DRAWING PROCEDURES A AND B ON THE ROOM TEMPERATURE MECHANICAL PROPERTIES OF Ni AND Ni-2ThO$_2$

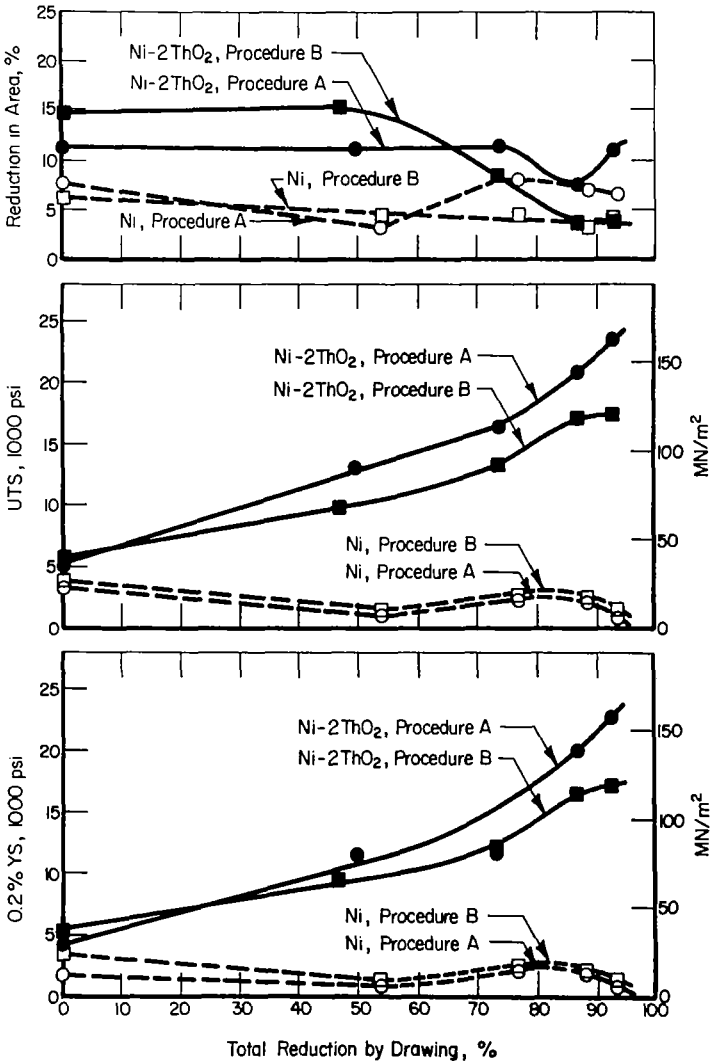

FIGURE 6. INFLUENCE OF DRAWING PROCEDURES A AND B ON THE MECHANICAL PROPERTIES OF Ni AND Ni-2ThO$_2$ AT 1093°C

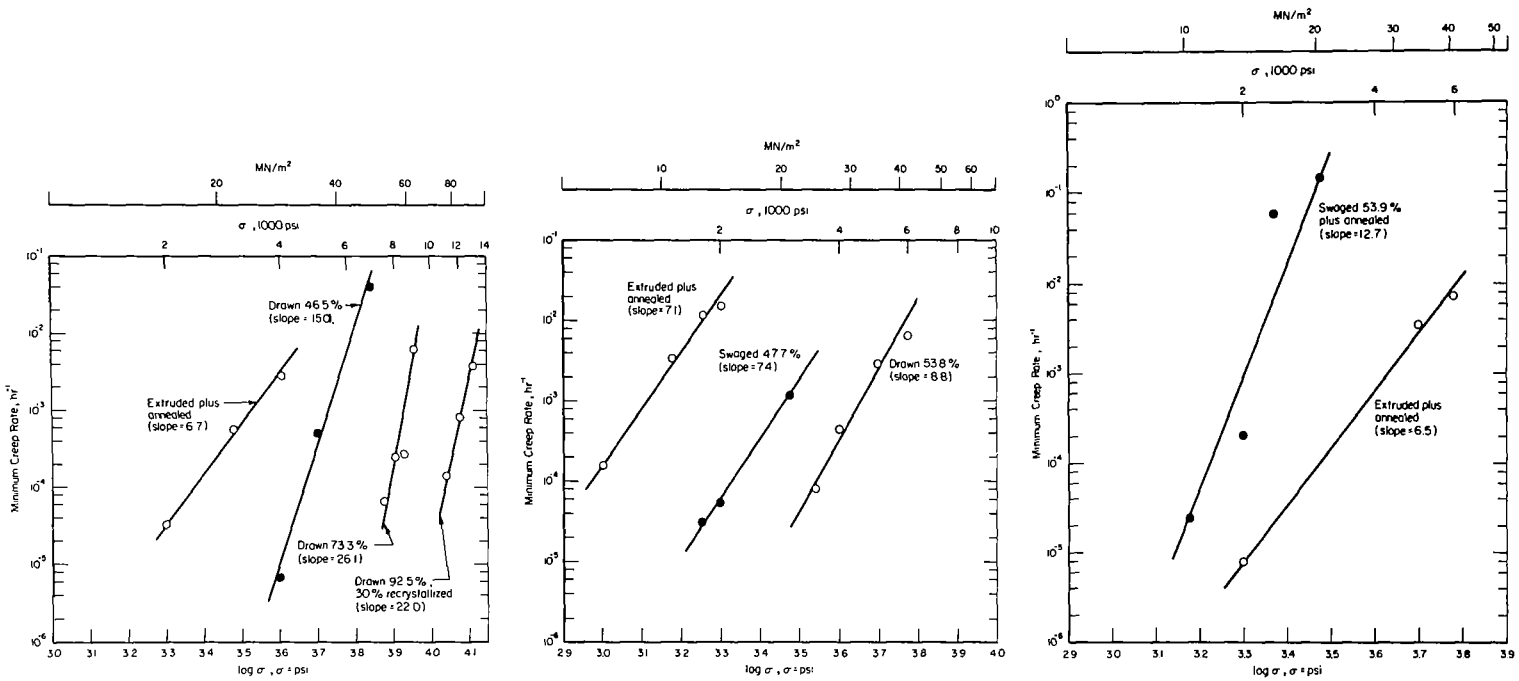

a. $Ni\text{-}2ThO_2$ b. $Ni\text{-}20Cr\text{-}2ThO_2$ c. $Ni\text{-}20Cr\text{-}10W\text{-}2ThO_2$

FIGURE 7. MINIMUM CREEP RATE OF THORIATED ALLOYS AT 1093°C AS A FUNCTION OF APPLIED STRESS

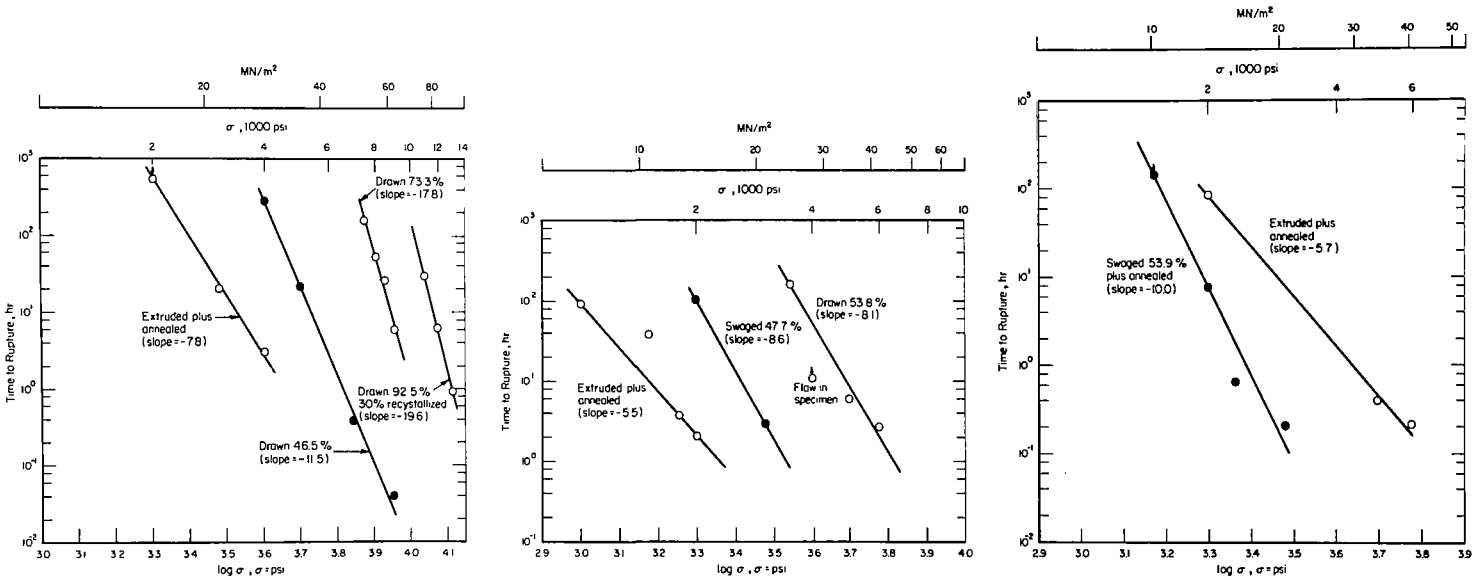

a. Ni-2ThO_2 b. Ni-20Cr-2ThO_2 c. Ni-20Cr-10W-2ThO_2

FIGURE 8. TIME TO RUPTURE AS A FUNCTION OF APPLIED STRESS FOR THORIATED ALLOYS CREEP TESTED AT 1093°C

exponents of 4 to 5 are common for creep of single crystals and pure polycrystalline metals, and exponents of 6 to 8 have been reported for recrystallized thoriated Ni alloys with a nearly equiaxed grain structure.[33-35] However, very high stress exponents are common for thermomechanically processed dispersion strengthened nickel alloys which have an elongated grain structure[23, 36, 37]. Thermomechanical processing of Ni-20Cr-2ThO_2 also increased the creep strength (Figures 7b and 8b), but the increase in stress exponent with TMP was small. Figures 7c and 8c show that the extruded plus annealed Ni-20Cr-10W-2ThO_2 was stronger than the alloy after TMP. These creep and rupture life results can be interpreted in terms of the microstructure, as is discussed later.

DISCUSSION

Room Temperature Deformation

The influence of TMP on room temperature strength is readily rationalized in terms of the Hall-Petch equation which relates the yield strength, σ, to the grain or substructure size, ℓ, by the equation:

$$\sigma = \sigma_o + k\ell^{-1/2} \quad . \tag{4}$$

Plots of yield strength versus $\ell^{-1/2}$ are shown in Figure 9 for Ni, Ni-2ThO_2, Ni-20Cr and Ni-20Cr-2ThO_2. Results from the present study are included together with data from previous investigations[1, 2, 13]. In drawn or swaged materials containing elongated closed cells, the value of ℓ was that dimension of the cell normal to the rod or wire axis; i.e., the width of the cell. Several features are apparent in Figure 9: (1) There is a convergence of the plots for a given base composition, i.e., the k values for the thoriated alloys are lower than those of the respective ThO_2-free alloys, and (2) The slopes of the Cr-containing alloys are higher than those of Ni and Ni-2ThO_2. The nonparallelism of the four plots in Figure 9 indicates that the direct additivity of strengthening mechanisms (e.g., solution strengthening, particle strengthening, and refinement of grain and substructure size) suggested by Hansen and Lilholt[38] is not correct. In Figure 9 the magnitude of strength increments due to Cr in solution and ThO_2 particles depends on the grain or cell size, ℓ.

At $\ell^{-1/2} = 0$, the particle strengthening contributions are 21,000 psi (145 MN/m^2) for Ni-2ThO_2 and 42,000 psi (290 MN/m^2) for Ni-20Cr-2ThO_2. The value for Ni-2ThO_2 corresponds exactly with the strengthening expected from the Orowan mechanism of hardening using the relation derived by Ashby[39,40]. However, the particle strengthening increment is about 1.7 times the expected Orowan strength contribution for Ni-20Cr-2ThO_2.

It is of interest to compare the relative room temperature hardening capability of second phase particles with that of grain or cell boundaries. The intersection at $\ell^{-1/2} = 0$ in Figure 9 shows that by starting with a single crystal of pure Ni, an increase of 21,000 psi (145 MN/m^2) in the 0.2% tensile yield strength can be achieved by adding 2.58 vol.% of randomly spaced ThO_2 particles having an average particle diameter of 0.02 μm, i.e., a mean planar edge-to-edge particle spacing of 0.134 μm. Also, from Figure 9 it is seen that the same increment in strength can be achieved by grain boundaries or tangled dislocation cells which have a spacing of 5.17 μm; i.e., $\ell^{-1/2} = 0.44\ \mu^{-1/2}$. Another way of examining this is to determine the expected increase in yield strength of pure Ni if the boundaries had the same spacing as particles in Ni-2ThO_2 (0.134 μm). Upon extrapolating the pure Ni results in Figure 9 to $\ell^{-1/2} = 2.73\ \mu^{-1/2}$, it is found that a yield strength increment of 133,500 psi (921 MN/m^2) would be realized, compared with the 21,000 psi (145 MN/m^2) achieved by particles which had the same edge-to-edge spacing as the boundaries. Thus, for a given spacing between boundaries or between particles, boundaries are more than six times as potent in raising the room temperature yield strength than are particles. A similar effect is obtained for Ni-20Cr and Ni-20Cr-2ThO_2.

Elevated Temperature Strength

In an attempt to ascertain whether the grain size and substructure refinement played a role in strengthening at high temperatures, the Hall-Petch analysis was applied to the Ni-2ThO_2 results for tensile tests at 1093 °C. Figure 10 is a plot of the 0.2% yield strength of Ni-2ThO_2 at 1093 °C as a function of $\ell^{-1/2}$. Here it is seen that there is a great deal of scatter, and thus no good correlation between yield strength and $\ell^{-1/2}$. For example, one point (open triangle) is for recrystallized TD Nickel with a coarse elongated grain structure, and the strength, 18,000 psi (124 MN/m^2), is the same as that for TD Nickel bar (closed circles) with a very fine nonrecrystallized elongated grain structure.

It was apparent, however, that the high temperature strength did relate to the shape of the grains or cells, and in fact, the yield strength and creep strength increased linearly with increasing grain aspect ratio (G.A.R.);

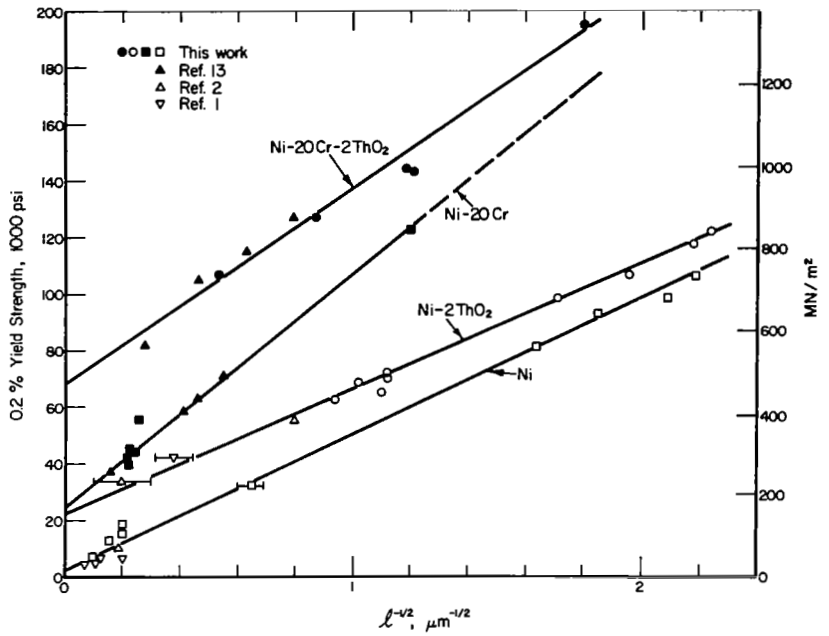

FIGURE 9. DEPENDENCE OF ROOM TEMPERATURE YIELD STRENGTH (0.2% OFFSET) OF Ni, Ni-2ThO_2, Ni-20Cr, AND Ni-20Cr-2ThO_2 ON GRAIN SIZE AND CELL SIZE PRODUCED BY DRAWING PROCEDURES A AND B

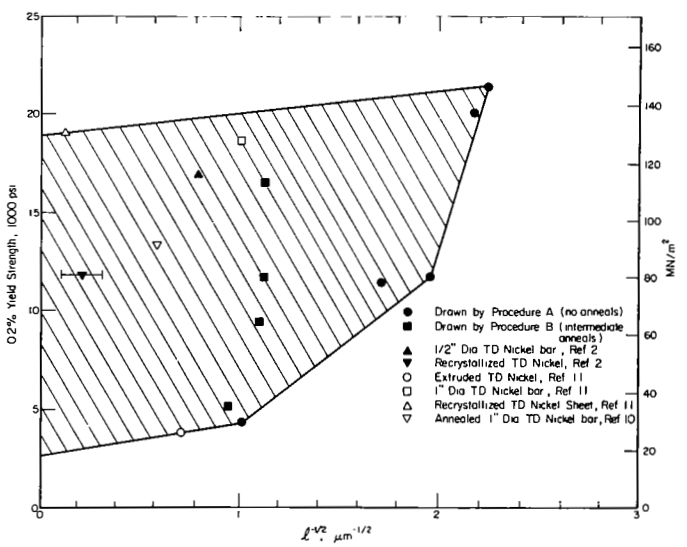

FIGURE 10. DEPENDENCE OF 0.2% OFFSET YIELD STRENGTH ON GRAIN OR CELL SIZE FOR Ni-2ThO_2 TESTED AT 1093°C

i.e., ratio of grain or cell length, L, to grain or cell width, ℓ. In Figure 11 the yield strength and creep strength at 1093°C are plotted versus L/ℓ for the materials examined in this study, together with previous results on non-recrystallized TD Nickel bar[2, 11, 23, 36], recrystallized TD Nickel which contained very coarse elongated grains[2, 11], TD NiCr sheet and foil which were recrystallized with coarse elongated grains[41, 42], Ni-Cr-W-ThO_2 alloys containing fine recrystallized grains[43], and recrystallized dispersion strengthened Ni-base superalloys[36, 44, 45]. It should be noted that in all of these studies the tensile stress axis was parallel to the elongated grain direction. From the available micrographs, it was not possible to determine the G.A.R. for all of the specimens examined in this study. In particular, if the ratios were $\gtrsim$ 12, it was impossible to obtain an accurate measure of the grain length, L. Also there is some uncertainty in the values of L/ℓ taken from the literature since usually only several measurements of the G.A.R. could be made from the published micrographs. An important feature of Figure 11 is that the TD Nickel bar data points (fine elongated non-recrystallized grains with a G.A.R. = 10-15 μm/1 μm) fall on the same plots as the recrystallized TD Nickel which had very coarse elongated grains, e.g., G.A.R. = 900 μm/100 μm. Under creep conditions (Figures 11b and 11c) the Ni-2ThO_2 points fit the same plots as the alloys containing Cr and W and the dispersion strengthened superalloys, which indicates that here the matrix composition has no significant effect on creep strength.

The influence of G.A.R. on high temperature strength can be formulated as follows. The yield strength or creep strength, σ, is given by

$$\sigma = \sigma_e + K(L/\ell - 1) \quad , \tag{5}$$

where σ_e is the strength for $L/\ell = 1$ (equiaxed grains) and K is a constant defined as the grain aspect ratio coefficient. Values of σ_e and K determined from Figure 11 are given in Table 3.

A physical interpretation of Figure 11 is that grain boundary sliding plays an important role in high temperature yielding. Wilcox and Clauer[23] previously suggested this to the case for high temperature creep of TD nickel bar, and Doble, et al[11] and Fraser and Evans[12] felt that grain boundary sliding was the predominant mechanism for yielding of Ni-ThO_2 alloys tensile tested at high temperatures. When most of the grain boundaries are parallel to the stress axis, i.e., a highly elongated microstructure, there is, on average, a low resolved shear stress on the boundaries. This minimizes the overall amount of sliding. The maximum sliding would occur when the grain aspect ratio was unity (equiaxed grains). It is probable that a coarse equiaxed structure would have better high temperature strength than a fine

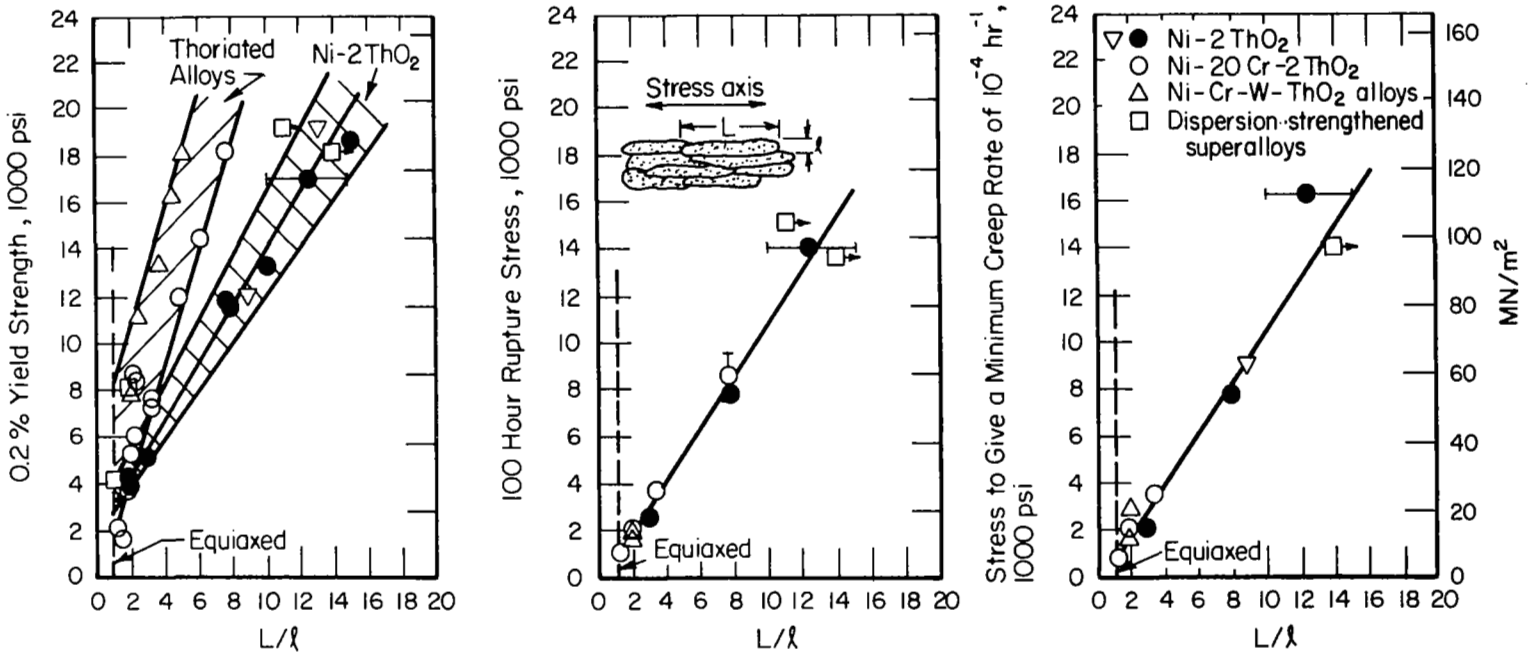

FIGURE 11. THE EFFECT OF GRAIN ASPECT RATIO, L/ℓ, IN DISPERSION-STRENGTHENED NICKEL ALLOYS ON STRENGTH PROPERTIES AT 1093°C

a. 0.2% offset yield strength; b. 100-hour rupture stress; and c. stress to give a minimum creep rate of 10^{-4} hr^{-1}. Open points are recrystallized and closed points are nonrecrystallized.

equiaxed structure, because having fewer boundaries would reduce the total amount of sliding. Thus, there can be a grain size effect at high temperatures and σ_e is probably not truly constant at a given temperature. It can be concluded, however, that when grains are elongated, the G.A.R. effect swamps any grain size effect.

At lower temperatures, approaching 0.5 T_m, or at much higher strain rates, it is expected that there would be a larger relative contribution of grain interior deformation to macroscopic yielding. Although there are not enough data presently available to quantitatively assess this in the case of thoriated nickel alloys, Figure 12 schematically depicts the anticipated behavior. Here the G.A.R. is plotted horizontally, and it is assumed that the grain width, ℓ, is constant. If this assumption were not made, then complications would arise because at higher rates and lower temperatures grain size strengthening would be superimposed on the grain aspect ratio effect. The interplay between grain size strengthening and deformation due to grain boundary sliding might be similar to the effects observed in dispersion strengthened zinc by Tromans and Lund.[46] In Figure 12a, there is no influence of aspect ratio at $T_1 < 0.5\ T_m$. This curve would be shifted to higher stresses as temperature is further lowered, or as ℓ was decreased at constant L/ℓ; i.e., the usual Hall-Petch strengthening. At $T_2 > 0.5\ T_m$ grain boundary sliding assumes some importance and here there is an effect of grain aspect ratio. At still higher temperatures, $T_3 >> 0.5\ T_m$, grain boundary sliding contributions to yielding become much more important, and the influence of L/ℓ on the yield strength is more pronounced. At these very high temperatures, grain width, ℓ is not significantly important from the Hall-Petch strengthening point of view, since most of the macroscopic yielding occurs by boundary sliding.

TABLE 3. VALUES OF THE GRAIN ASPECT RATIO COEFFICIENT, K, AND EQUIAXED GRAIN STRENGTH, σ_e, FOR THORIATED NICKEL ALLOYS DEFORMED AT 1093°C IN TENSION AND CREEP

	$Ni\text{-}2ThO_2$		Dispersion Strengthened Ni-20Cr-base Alloys	
	K	σ_e	K	σ_e
0.2% yield strength	1200 psi (8.3 MN/m^2)	3000 psi (20.7 MN/m^2)	2800 psi (19.3 MN/m^2)	2000-4000 psi (13.8-27.6 MN/m^2)
Stress for 100-hr rupture life	1100 psi (7.6 MN/m^2)	1000 psi (6.9 MN/m^2)	1100 psi (7.6 MN/m^2)	1000 psi (6.9 MN/m^2)
Stress to give a minimum creep rate of $10^{-4}hr^{-1}$	1100 psi (7.6 MN/m^2)	1000 psi (6.9 MN/m^2)	1100 psi (7.6 MN/m^2)	1000 psi (6.9 MN/m^2)

Similarly, Figure 12b reveals the anticipated effects of strain rate at $T >> 0.5\ T_m$. For very high rates of deformation, $\dot{\epsilon}_1$, grain boundary sliding may not occur, and hence there is no effect of aspect ratio on yield strength. Here there would be an effect on strength due to grain width, ℓ. At progressively lower strain rates, $\dot{\epsilon}_2$ and $\dot{\epsilon}_3$, sliding would become more pronounced, and there would be a larger influence of G.A.R. on yield strength.

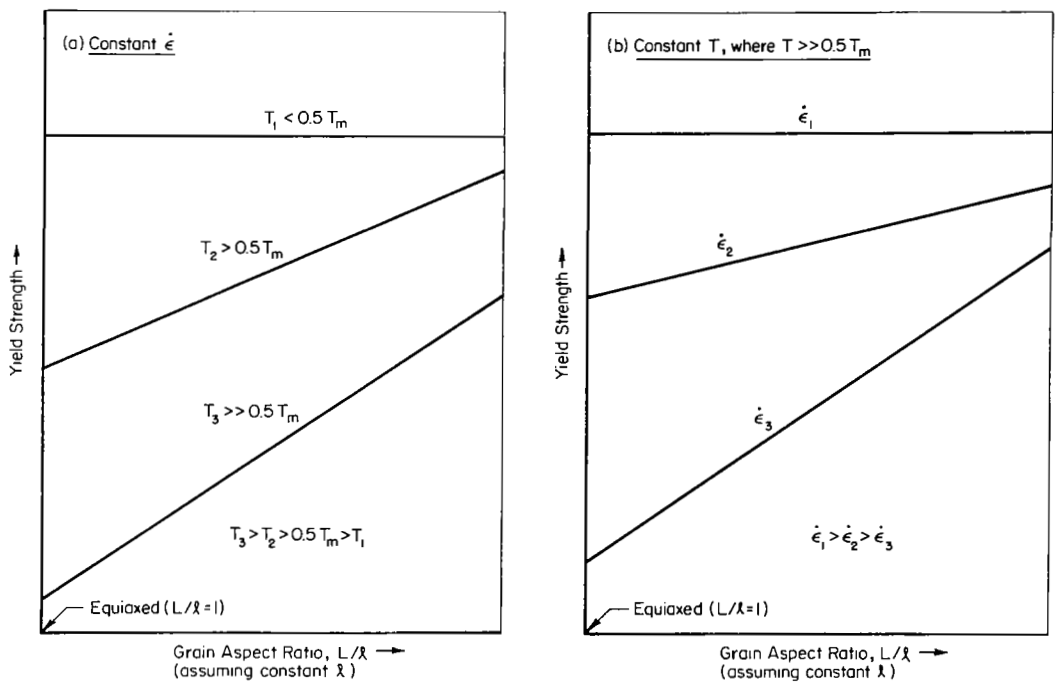

FIGURE 12. SCHEMATIC PLOTS SHOWING HOW TEST TEMPERATURE AND STRAIN RATE MAY INFLUENCE THE RELATION BETWEEN YIELD STRENGTH AND GRAIN ASPECT RATIO, L/ℓ, in Ni-ThO_2-BASE ALLOYS

The grain elongation effect should be apparent at temperatures above ~$0.5\ T_m$ (~600 °C for dispersion strengthened Ni alloys) since here there can be a significant contribution of grain boundary sliding to the total deformation. At 1093 °C it appears that sliding plays a dominant role. Grain boundary sliding requires accommodation deformation by diffusional processes or dislocation motion within grains. At lower temperatures, approaching $0.5\ T_m$, or at higher strain rates, it is expected that there would be a larger relative contribution to the accommodation deformation by dislocation motion, whereas at higher temperatures or slower strain rates, the contribution by diffusion would become increasingly important. This may explain

why in Figure 11a the yield strength of thoriated alloys containing Cr and W is greater than that of Ni-ThO_2. The tensile strain rates are high ($\sim 10^{-3}$ to $10^{-4} sec^{-1}$) compared with creep rates (10^{-5} to $10^{-9} sec^{-1}$). Thus the accommodation deformation in yielding may be predominantly by dislocation motion within grains and the increment of solid solution strengthening by Cr and W would be realized. However, the solute elements should not significantly influence diffusion and thus the tendency for diffusion accommodation of grain boundary sliding during creep should not produce a solution strengthening effect. This in fact appears to be the case (Figures 11b and 11c).

The conclusion that an elongated grain structure is desirable for high temperature strength is not new. For example, workers in the lamp filament industry have known for many years that doped tungsten, which recrystallizes to a coarse elongated grain structure, is far superior to undoped tungsten, which recrystallizes with an equiaxed grain structure. The benefit of doping is derived in part from enhanced creep resistance due to the elongated interlocking grain structure. Also, Ver Snyder and Guard[47] obtained directional grain structures in a cast Ni-Cr-Al alloy, and found improved high temperature ductility and creep rupture behavior compared with the same alloy having an equiaxed grain structure. Bourne, et al[48] dispersion strengthened Pt and Pt alloys with a number of oxides and carbides. They produced stable elongated grains by thermomechanical processing, with grain aspect ratios as high as 12.5, and they found that high temperature creep rupture life increased with increasing G.A.R. For example, in a thermomechanically processed Pt-0.04% TiC alloy they found the following results: at 1400°C and 700 psi (4.8 MN/m^2) t_r = 800 hours for L/ℓ = 5 and t_r = 1200 hours for L/ℓ = 12.5. Recently, Benjamin[44] and Benjamin and Cairns[36] reported a new superalloy development involving "mechanical alloying" which allowed them to combine γ' hardening for low temperature strength with oxide dispersion strengthening for high temperature strength. Their material was hot extruded, and when recrystallized it had a coarse, very elongated grain structure. In this condition, the ultimate tensile strength at 1093°C was equivalent to that of TD Nickel bar. Prior to this development, Cook, et al[45], produced in sheet form a Ni-base alloy strengthened by γ' which also contained ThO_2 particles. Their material in the heat treated condition had low temperature strength equivalent to Nimonic 80-A, but at high temperatures ($\gtrsim$ 950°C) the usual ThO_2 particle strengthening was not achieved. The microstructure contained fine, nearly-equiaxed grains and the primary mode of deformation at high temperatures was probably grain boundary sliding. Because pronounced sliding took place at relatively low stresses, compared with that required to produce macroscopic matrix yielding, the potential ThO_2 strengthening was not utilized.

At this point, it is useful to compare the present results on Ni-ThO_2 with the work of previous investigations[7, 11, 12] which have related

thermomechanical processing by drawing and swaging to room temperature and high temperature strength properties. This is done in Figure 13, which shows plots of ultimate strength at 25, 871, and 1093 °C as a function of reduction by drawing or swaging. Ultimate strength, rather than yield strength, is plotted since several of the previous investigations reported only this property. The room temperature strength of Ni-2ThO_2 drawn by Procedure A increases with increasing drawing strain in the same general fashion as the earlier work of Tracey and Worn[7], and this is associated with substructure refinement. However, the strength at 871 °C[12] and 1093 °C[11] behaves somewhat differently from the results obtained in this investigation. Figure 13 shows that after ~70% reduction by drawing, the strength at 871 °C remains constant with further working. Also, after swaging, the strength at 1093 °C remains constant for strains greater than ~85%. However, the strengths at 1093 °C of Ni-2ThO_2 drawn by Procedures A and B in this study continue to increase with increasing drawing strains up to ~93%. A possible explanation for this difference is that Fraser and Evans[12] and Doble, et al[11] reached a constant grain aspect ratio at high working reductions, but this did not occur in the present study.

In a previous investigation, Wilcox and Jaffee[2] found that ThO_2 particles in recrystallized TD Nickel produced an increase in yield strength, compared with pure polycrystalline nickel, over the entire temperature range 25 to 1200 °C. The increase in strength above that of pure Ni was 22,000 (152 MN/m^2) psi at 25 °C and 9000 psi (62.1 MN/m^2) at 1200 °C. The recrystallized TD Nickel had coarse elongated grains, with an $L/\ell = 8.7$. Wilcox and Jaffee rationalized the increase in yield strength over the entire temperature range in terms of the Orowan mechanism. However, based on the findings of the present study, it now appears that above ~600 °C, where grain boundary sliding becomes important, the agreement with the Orowan mechanism may have been fortuitous. For example, if the recrystallized TD Nickel had a drastically different grain aspect ratio, say $L/\ell = 2$, then the yield strength would have been ~67% lower at 1093 °C (Figure 11a), and agreement with the Orowan mechanism at this temperature would not have been realized.

The above discussion should not be construed to indicate that dispersion (or even substructure) strengthening is not important at high temperatures. However, the grain aspect ratio must be large, preferably > 10, before these strengthening mechanisms can be effectively utilized to make matrix yielding more difficult. It appears that the major role of ThO_2 particles in improving high temperature strength is indirect and is associated with the particles stabilizing an elongated grain structure. The benefit of thermomechanical processing on high temperature strength arises from the development of high grain aspect ratios.

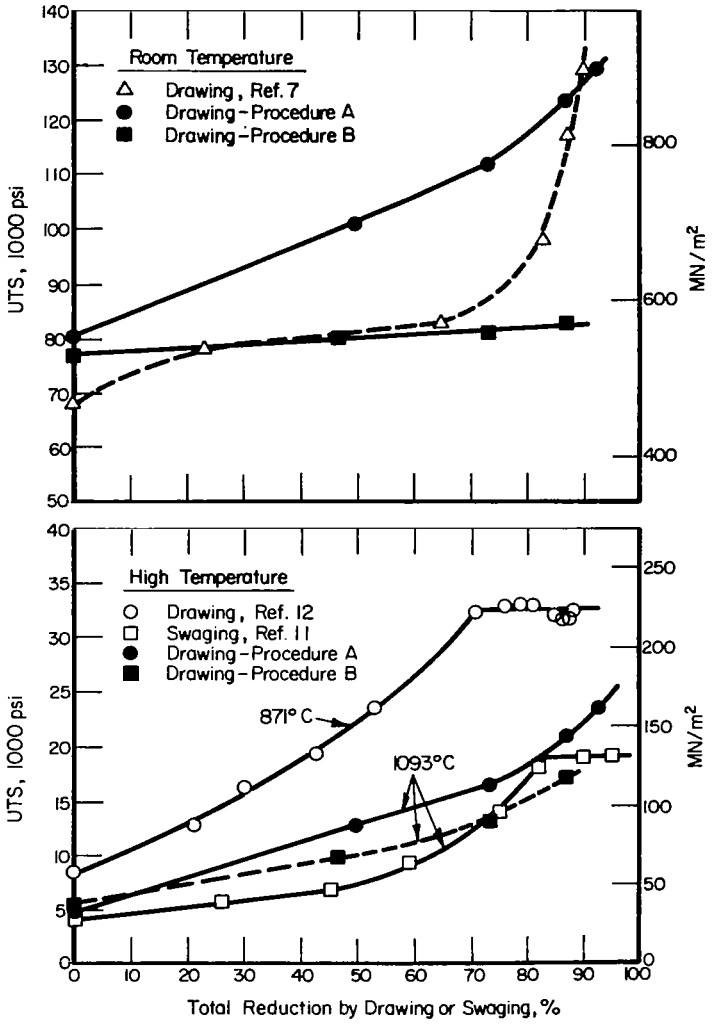

FIGURE 13. ROOM-TEMPERATURE AND HIGH-TEMPERATURE STRENGTH OF Ni-2ThO_2 ALLOYS AS A FUNCTION OF REDUCTION BY DRAWING OR SWAGING

Results of this work are compared with those of previous investigators. In each case the starting material was extruded bar.

CONCLUSIONS

(1) Thermomechanical processing (TMP) of dispersion strengthened nickel alloys produces various microstructures which influence subsequent room temperature and high temperature mechanical properties. One important microstructural feature observed was the elongated grain structure. Under the conditions employed here this was always present in Ni-2ThO_2. However, in dispersion alloys containing Cr the materials often recrystallized to a fine nearly equiaxed grain structure.

(2) At room temperature substructure refinement of thoriated and ThO_2-free alloys results in strengthening by the usual Hall-Petch relation. Refining the substructure of Ni or Ni-20Cr by TMP to a cell spacing equivalent to the interparticle spacing in Ni-2ThO_2 and Ni-20Cr-2ThO_2 increases the room temperature yield strength five to six times more than dispersion strengthening alone.

(3) At 1093 °C it was shown that the yield strength, 100 hour creep rupture life, and stress to produce a creep rate of $10^{-4}hr^{-1}$ all increase linearly with increasing grain aspect ratio, L/ℓ, where L = grain length and ℓ = grain width. This correlation holds for Ni-2ThO_2, Ni-20Cr-2ThO_2, Ni-Cr-W-ThO_2 alloys, and dispersion strengthened Ni-base superalloys, and emphasizes the importance of having a large grain aspect ratio for improved high temperature strength.

(4) The grain aspect ratio effect is attributed to the fact that grain boundary sliding is the major mode of deformation in dispersion strengthened Ni alloys at high temperatures. When testing is performed such that the tension axis is parallel to the fiber axis then increasing the L/ℓ lowers, on average, the shear stress on boundaries, and this in turn reduces the amount of grain boundary sliding.

REFERENCES

1. M. Von Heimendahl and G. Thomas, Trans. AIME, 230, 1520 (1964).

2. B. A. Wilcox and R. I. Jaffee, First International Conference on the Strength of Metals and Alloys, Suppl. to Trans. Japan Inst. Met., 9, 575 (1968).

3. D. W. Ashall and P. E. Evans, Met. Sci. J., 2, 96 (1968).

4. D. Webster, Trans. ASM, 62, 936 (1969).

5. R. Scharwächter, Second International Conference on the Strength of Metals and Alloys, American Society for Metals, Metals Park, Ohio, 1970, p. 644.

6. D. K. Worn and S. F. Marton, Powder Metallurgy, Interscience Publishers, New York, 1961, p. 309.

7. V. A. Tracey and D. K. Worn, Powder Metallurgy (No. 10), 34 (1962).

8. R. Murphy and N. J. Grant, Powder Metallurgy (No. 10), 1 (1962).

9. R. W. Fraser, B. Meddings, D. J. I. Evans, and V. N. Machiw, Modern Developments in Powder Metallurgy, H. H. Hausner, Ed., Plenum Press, New York, 1966, p. 87.

10. G. S. Doble and R. J. Quigg, Trans. AIME, 233, 410 (1965).

11. G. S. Doble, L. Leonard, and L. J. Ebert, "The Effect of Deformation on Dispersion Hardened Alloys", Final Report on NASA Grant NGR 36-033-094, Nov., 1967.

12. R. W. Fraser, and D. J. I. Evans, Oxide Dispersion Strengthening, G. S. Ansell, et al, Eds., Gordon and Breach, New York, 1968, p. 375.

13. D. Webster, Trans. AIME, 242, 640 (1968).

14. M. C. Inman, K. M. Zwilsky, and D. H. Boone, Trans. ASM, 57, 701 (1964).

15. P. B. Mee and R. A. Sinclair, J. Inst. Met., 94, 319 (1966).

16. E. R. Kimmel and M. C. Inman, Trans. ASM, 62, 390 (1969).

17. A. Bassi, G. Camona, M. Conserva, and P. Fiorini, Mem. Sci. Rev. Met., 64, 547 (1967).

18. L. E. Murr and H. R. Vydyanath, Acta Met., 18, 1047 (1970).

19. R. K. Hotzler and L. S. Castleman, Trans. AIME, 242, 750 (1968).

20. D. H. Killpatrick, Second International Conference on the Strength of Metals and Alloys, American Society for Metals, Metals Park, Ohio, 1970, p. 649.

21. D. H. Killpatrick, "Recrystallization of TD NiCr Bar", McDonnell Douglas Rept. No. WD 1636, June, 1971.

22. G. S. Ansell, Oxide Dispersion Strengthening, G. S. Ansell, et al, Eds., Gordon and Breach, New York, 1968, p. 61.

23. B. A. Wilcox and A. H. Clauer, Trans. AIME, 236, 570 (1966).

24. D. H. Killpatrick, A. Phillips, and V. Kerlins, Trans. AIME, 242, 1657 (1968).

25. R. J. Olsen and G. S. Ansell, Trans. ASM, 62, 711 (1969).

26. R. J. Olsen, G. Judd, and G. S. Ansell, Met. Trans., 2, 1353 (1971).

27. J. D. Embury and R. M. Fisher, Acta Met., 14, 147 (1966).

28. J. D. Embury, A. S. Keh, and R. M. Fisher, Trans. AIME, 236, 1252 (1966).

29. V. K. Chandhok, A. Kasak, and J. P. Hirth, Trans. ASM, 59, 288 (1966).

30. G. Langford and M. Cohen, Trans. ASM, 62, 623 (1969).

31. B. A. Wilcox and A. Gilbert, Acta Met., 15, 601 (1967).

32. E. S. Meieran and D. A. Thomas, Trans. AIME, 233, 937 (1965).

33. A. H. Clauer and B. A. Wilcox, Met. Sci. J., 1, 86 (1967).

34. B. A. Wilcox and A. H. Clauer, Met. Sci. J., 3, 26 (1969).

35. B. A. Wilcox and A. H. Clauer, Oxide Dispersion Strengthening, G. S. Ansell, et al, Eds., Gordon and Breach, New York, 1968, p. 323.

36. J. S. Benjamin and R. L. Cairnes, Modern Developments in Powder Metallurgy, Vol. 5, H. H. Hausner, Ed., Plenum Press, New York, 1971, p. 47.

37. B. A. Wilcox, A. H. Clauer, and W. S. McCain, Trans. AIME, 239, 1791 (1967).

38. N. Hansen and H. Lilholt, Modern Developments in Powder Metallurgy, Vol. 5, H. H. Hausner, Ed., Plenum Press, New York, 1971, p. 339.

39. M. F. Ashby, Oxide Dispersion Strengthening, G. S. Ansell, et al, Eds., Gordon and Breach, New York, 1968, p. 143.

40. M. F. Ashby, Physics of Strength and Plasticity, A. Argon, Ed., The M.I.T. Press, Cambridge, Mass., 1969, p. 113.

41. D. B. Arnold and L. J. Klingler, "Dispersion-Strengthened Nickel-Base Alloys", Oxide Dispersion Strengthening, G. S. Ansell, T. D. Cooper, and F. V. Lenel, Eds., Gordon and Breach, New York (1968), p. 611.

42. P. G. Baily, "A Manufacturing Process for Thin Sheet and Foil of TD Nickel-Chromium Alloy", AFML-TR-68-87, April, 1968.

43. L. F. Norris, B. W. Kushnir, and R. W. Fraser, "Improvement of the Properties of Dispersion Strengthened Nickel-Chromium Alloys", AFML-TR-68-67, March, 1968.

44. J. S. Benjamin, Met. Trans., 1, 2943 (1970).

45. R. C. Cook, R. H. MacDonald, and L. F. Norris, "Development of Precipitation Hardened Dispersion Strengthened Nickel-Chromium Alloys", AFML-TR-69-166, June, 1969.

46. D. Tromans and J. A. Lund, Trans. ASM, 59, 672 (1966).

47. F. L. Ver Snyder and R. W. Guard, Trans. ASM, 52, 485 (1960).

48. A. A. Bourne, J. C. Chaston, A. S. Darling, and G. C. Bond, "Methods of Improving the Mechanical Properties of Metals and Their Alloys", British Patent No. 1,134,492, November 27, 1968.

NASA-Langley, 1972 — 17 E-6790